

## SHINGLE OF A ROOF – CU ALLOY – MODERN TIMES – SWITZERLAND

<b>Artefact name</b>	Shingle of a roof
<b>Authors</b>	Marianne. Senn (EMPA, Dübendorf, Zurich, Switzerland) & Christian. Degriigny (HE-Arc CR, Neuchâtel, Neuchâtel, Switzerland)
<b>Url</b>	/artefacts/220/

### ∨ The object

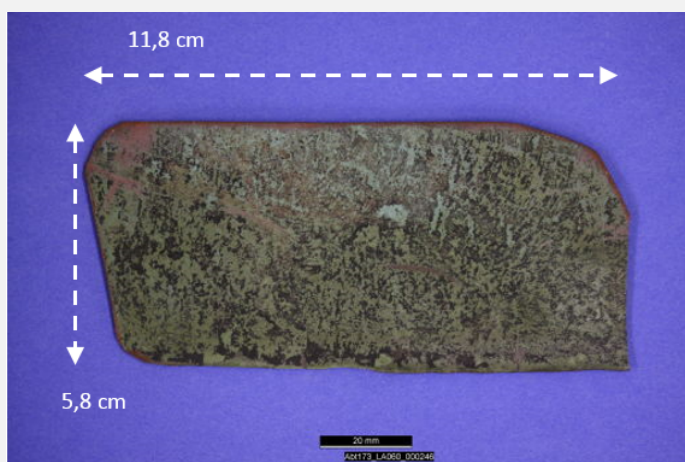


Fig. 1: Copper alloy shingle, internal side,

Credit HE-Arc CR.

### ∨ Description and visual observation

<b>Description of the artefact</b>	Shingle, slightly curved, the internal side is covered with green and black corrosion products distributed heterogeneously (Fig. 1). The external side shows a regular dark green corrosion crust. Dimensions: L = 11.8cm; W = 5.8cm.
<b>Type of artefact</b>	Architectural element
<b>Origin</b>	Roof of the abbey of St. Gallen, Sankt Gallen, Saint Gallen, Switzerland
<b>Recovering date</b>	None
<b>Chronology category</b>	Modern Times
<b>chronology tpq</b>	<input type="text" value="1780"/> A.D. ▾
<b>chronology taq</b>	<input type="text" value=""/> ---- ▾
<b>Chronology comment</b>	1780
<b>Burial conditions / environment</b>	Outdoor atmosphere
<b>Artefact location</b>	Conservation Department of the Musées d'art et d'histoire, Genève, Geneva
<b>Owner</b>	Abbey of St Gallen, Sankt Gallen, Saint Gallen

Inv. number None  
Recorded conservation data Not conserved

Study area(s)



Fig. 2: showing the location of sampling area,

Credit HE-Arc CR.

Binocular observation and representation of the corrosion structure

Stratigraphic representation: none

MiCorr stratigraphy(ies) – Bi

Sample(s)

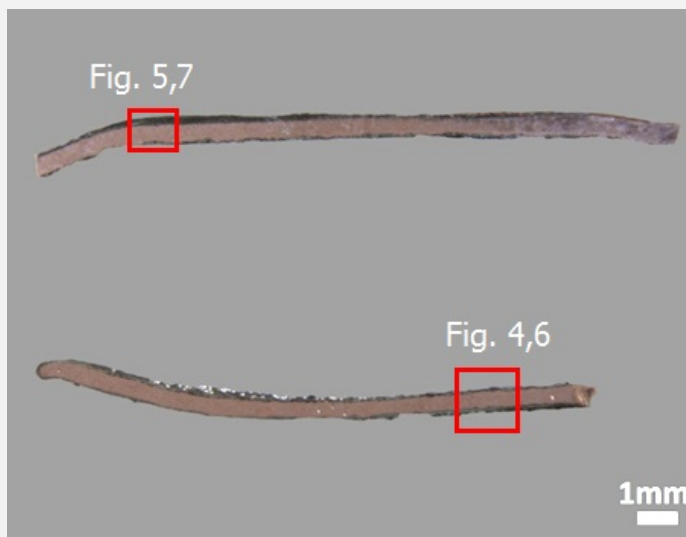


Fig. 3: Micrograph of the cross-sections showing the locations of Figures 4 to 7,

Credit HE-Arc CR.

Description of sample

The polished samples show a well-preserved metal surface with a thin corrosion crust (Fig. 3). T = 0.5mm.

<b>Alloy</b>	Cu Alloy
<b>Technology</b>	Rolled (probably hot rolling) and annealed
<b>Lab number of sample</b>	MAH-98-257
<b>Sample location</b>	Empa (Marianne Senn)
<b>Responsible institution</b>	Conservation Department of the Musées d'art et d'histoire, Genève, Geneva
<b>Date and aim of sampling</b>	2009, integration of sample to the MIFAC-Métal project

#### ∨ Analyses and results

##### *Analyses performed:*

Metallography (etched with ferric chloride reagent), Vickers hardness testing, LA-ICP-MS, SEM/EDX, XRD, Raman spectroscopy.

#### ∨ Non invasive analysis

#### ∨ Metal

The remaining metal is a copper alloy (Table 1). The evenly distributed inclusions observed under SEM, SE-mode, are either light-grey or white (Fig. 4). The oval shape of the light-grey inclusions is due to deformation, probably hot rolling (common in the 18th century). Under polarised light they look red (Fig. 6) and their analysis reveals a composition similar to cuprite/Cu<sub>2</sub>O (Table 2). The white inclusions are rich in Pb and are remnants of the refining process (Table 2). The etched copper shows a structure of polygonal and twinned grains (Fig. 5). The grain size is variable. The average hardness of the metal is about HV1 70.

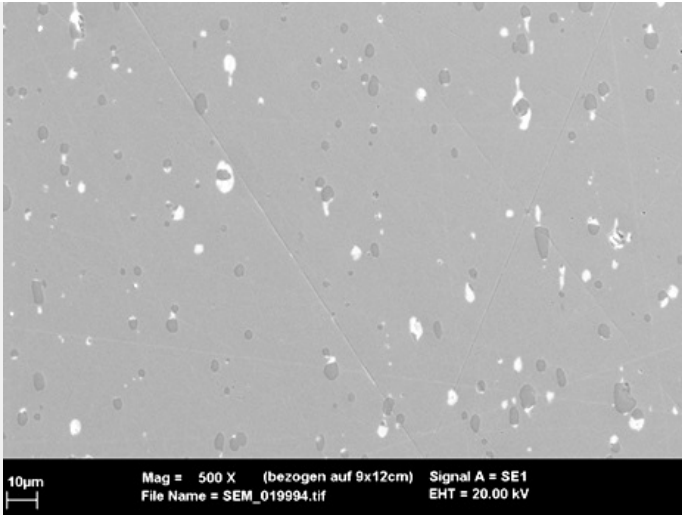
Elements	Cu	Pb	As	Sb	Ag	Bi	Sn	Zn	Ni	Fe	Co
mass%	99	0.7	0.1	0.1	0.05	<	<	<	<	<	<
RSD %	0.3	25	20	7	4						

Table 1: Chemical composition of the metal. Method of analysis: LA-ICP-MS, Laboratory of Basic Aspects of Analytical Chemistry at the Faculty of Chemistry, University of Warsaw, PL.

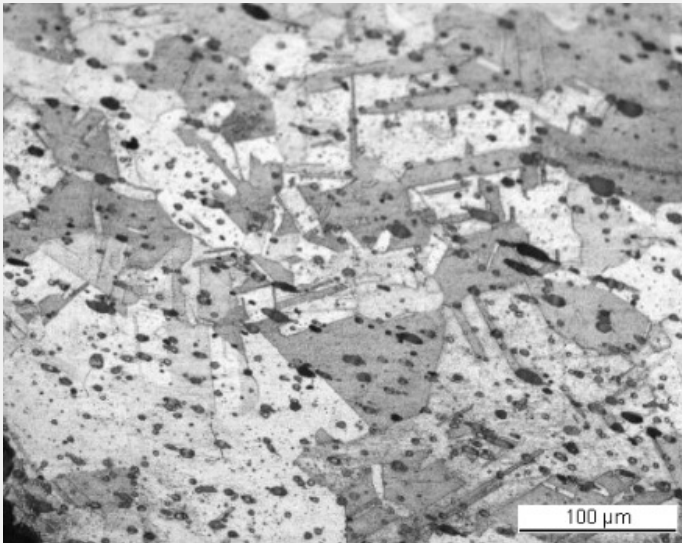
Elements	O	Cu	Pb	As	Sb	Total
Light-grey inclusion	9.8	86	<	<	<	96
White inclusion	9	9.1	68	5.1	2.6	94

Table 2: Chemical composition (mass %) of the inclusions in the metal (from Fig. 4). Method of analysis: SEM/EDX, Laboratory of Analytical Chemistry, Empa.

Fig. 4: SEM image, SE-mode, of the metal sample from Fig. 3 (detail). Light-grey and white inclusions are distributed evenly,



Credit HE-Arc CR.



Credit HE-Arc CR.

Fig. 5: Micrograph of the metal sample from Fig. 3 (detail), etched, bright field. The metal shows a structure of polygonal and twinned grains. Cuprite inclusions appear as dark spots,

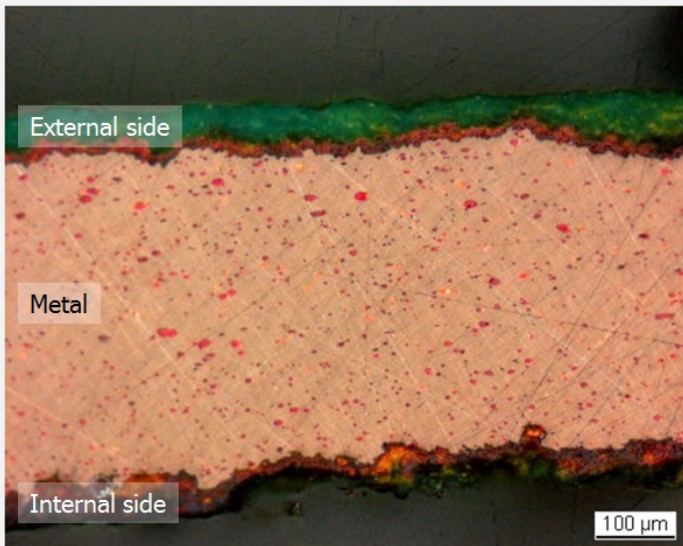
<b>Microstructure</b>	Polygonal and twinned grains, elongated inclusions
<b>First metal element</b>	Cu
<b>Other metal elements</b>	

∨ Corrosion layers

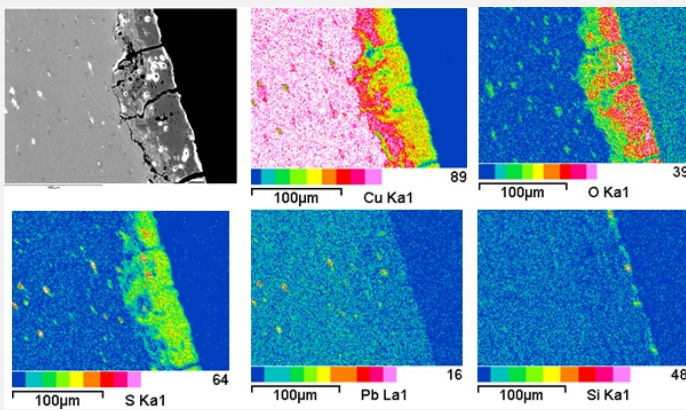
The corrosion crusts of the external and internal sides are distinctively different (Fig. 6). On the internal side an irregular red-orange corrosion layer has developed and pitting corrosion has occurred. The more uniform corrosion layers on the external side are composed of a red-orange layer, followed by a thicker green outer layer. In some areas, dark-red corrosion products can be observed between the green and red-orange sub-layers. The same dark-red sub-layer can be seen in areas on the internal side covering the red-orange corrosion products. The red-orange corrosion layer has a chemical composition similar to cuprite/ $\text{Cu}_2\text{O}$ , while the green layer contains Cu, S and O and is enriched on its upper surface with Si (Table 3 and Fig. 7). XRD analysis of the corrosion products on the external side of another shingle fragment from the same roof identified brochantite/ $\text{Cu}_4\text{SO}_4(\text{OH})_6$  and cuprite as corrosion products (Rapport d'analyse no MAH 98-257). These results are confirmed by Raman spectroscopy of the external side of this sample where the same compounds were clearly identified (Figs. 8 and 9).

Elements	O	Cu	S	Total
CP1e	20	59	6.2	85
CP2i	11	86	<	97

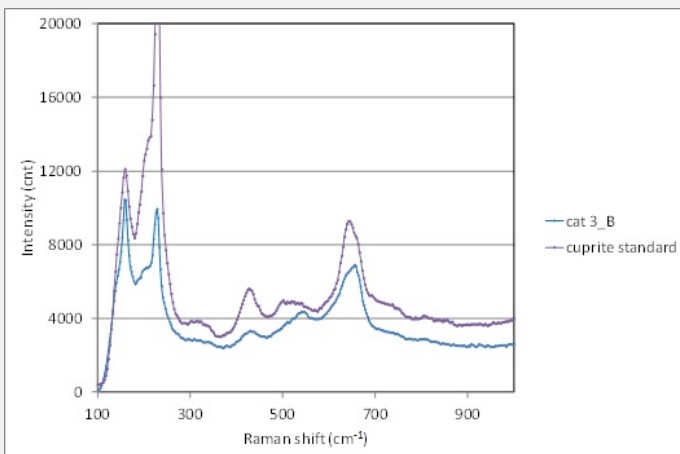
Table 3: Chemical composition (mass %) of the corrosion layers of the external side. Method of analysis: SEM/EDX, Laboratory of Analytical Chemistry, Empa.



Credit HE-Arc CR.



Credit HE-Arc CR.



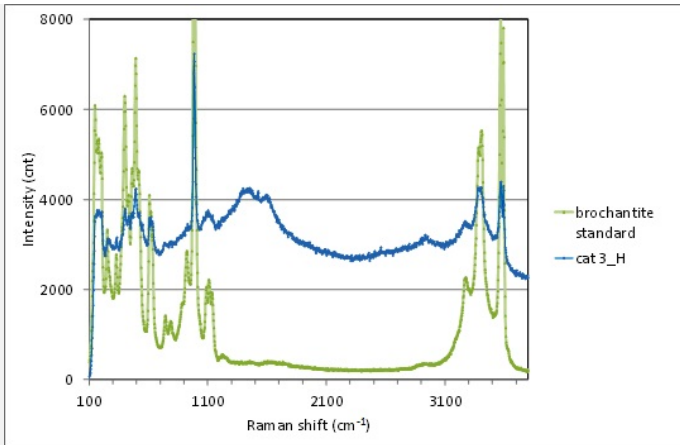
Credit HE-Arc CR.

Fig. 6: Micrograph of the metal sample from Fig. 3, polarised light. External side: the regular corrosion crust with outer green, inner red-orange corrosion products and intermediate dark-red corrosion products. Internal side: the irregular corrosion crust with inner red-orange and outer dark-red corrosion products,

Fig. 7: SEM image, SE-mode, and elemental chemical distribution of the selected area of Fig. 3 (rotated image, detail). Method of examination: SEM/EDX, Laboratory of Analytical Chemistry, Empa.

Fig. 8: Raman spectrum of the red-orange inner corrosion layer of the external side (cat3\_B) compared to a cuprite standard spectrum. Settings: laser wavelength 532nm, acquisition time 100s, one accumulation, filter D2 (0.75-0.8 mW), hole 500, slit 80, grating 600. Method of analysis: Raman spectroscopy, Lab Swiss National Museum, Affoltern a. Albis ZH,

Fig. 9: Raman spectrum of the green outer corrosion layer of the external side (cat3\_H) compared to a brochantite standard spectrum. Settings: laser wavelength 532nm, acquisition time 100s, one accumulation, filter D2 (0.75-0.8 mW), hole 500, slit 80, grating 600. The peak indicated with an arrow on the cat3\_H spectrum is due to fluorescence. Method of analysis: Raman spectroscopy, Lab Swiss National Museum, Affoltern a. Albis ZH,



Credit HE-Arc CR.

**Corrosion form** Uniform - pitting

**Corrosion type** Type I (Robbiola)

✧ MiCorr stratigraphy(ies) – CS

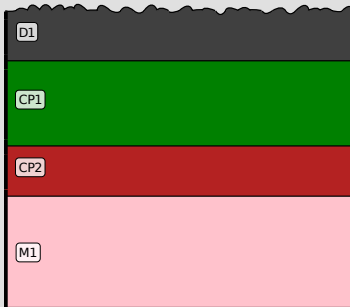


Fig. 4: Stratigraphic representation of the object in cross-section using the MiCorr application. This representation can be compared to Fig. 7.

✧ Synthesis of the binocular / cross-section examination of the corrosion structure

Corrected stratigraphic representation: none

✧ Conclusion

The copper shingle was rolled (probably hot rolling) and annealed to recover the ductility of the original material. The metal is covered on its external side by a typical “urban outdoor” patina consisting of copper sulphate (brochantite/ $\text{Cu}_4(\text{OH})_6\text{SO}_4$ ) formed on top of a cuprite/ $\text{Cu}_2\text{O}$  layer. The surface of the internal side, protected from the diluted sulphuric acid present in urban rain water, has developed only a cuprite layer. The silica present in the brochantite on the external side is due to airborne particle pollution. The corrosion is probably of type 1 after Robbiola et al. 1998.

✧ References

*References on object and sample*

1. Rapport d'analysen° MAH 98-257. Laboratoire Musées d'art et d'histoire, Genève. The report describes a sample from another shingle.

*References on analytic methods and interpretation*

2. Robbiola, L., Blengino, J-M., Fiaud, C. (1998) Morphology and mechanisms of formation of natural patinas on archaeological Cu-Sn alloys,

Corrosion Science, 40, 12, 2083-2111.

3. Selwyn, L. (2004) Metals and Corrosion: A Handbook for the Conservation Professional, Ottawa, ON: Canadian Conservation Institute, 68-70.

4. Stöckle, B., Mach, M. and Krätschmer, A. (1997) La durabilité des couvertures en cuivre selon les conditions environnementales. Résultat de l'UN/ECE-Programme d'exposition climatique, Les couvertures métalliques, matériaux et techniques, Les cahiers de la section française de l'ICOMOS, Paris, 129-135.

5. Welter, J-M. (2007) La couverture en cuivre en France: une promenade à travers les siècles, Le métal dans l'architecture, Monumental, 104-112.